

Before and After: How has the SNO neutral current measurement changed things?

John N. Bahcall

School of Natural Sciences, Institute for Advanced Study, Princeton, NJ 08540
E-mail: jnb@ias.edu

M. C. Gonzalez-Garcia

Theory Division, CERN, CH-1211, Geneva 23, Switzerland,
C.N. Yang Institute for Theoretical Physics
State University of New York at Stony Brook
Stony Brook, NY 11794-3840, USA,
and Instituto de Física Corpuscular, Universitat de València – C.S.I.C.
Edificio Institutos de Paterna, Apt 22085, 46071 València, Spain
E-mail: concepcion.gonzalez-garcia@cern.ch

Carlos Peña-Garay

Instituto de Física Corpuscular, Universitat de València – C.S.I.C.
Edificio Institutos de Paterna, Apt 22085, 46071 València, Spain
E-mail: penya@ific.uv.es

ABSTRACT: We present “Before and After” global oscillation solutions, as well as predicted “Before and After” values and ranges for eight future solar neutrino observables. The “Before” case includes all solar neutrino data (and some theoretical improvements) available prior to April 20, 2002 and the “After” case includes, in addition, the new SNO data on the CC, NC, and day-night asymmetry. The LMA solution is the only currently allowed MSW oscillation solution at a C.L. of 98.8%. The LOW solution is allowed only at 2.5σ , SMA at 3.7σ , and pure sterile oscillations at 5.4σ . Small mixing angles are “out” (pure sterile is “way out”); MSW with large mixing angles is definitely “in.” Vacuum oscillations are allowed, but not robustly, at 2.1σ . Precise maximal mixing is excluded at 3.2σ for MSW solutions and at 2.8σ for vacuum solutions. Most of the predicted values for future observables for the BOREXINO, KamLAND, and future SNO measurements are changed only by minor amounts by the inclusion of the recent SNO data. In order to evaluate the effects of spectral energy distortions, we have performed calculations both with and without using the detailed experimental data provided by the SNO collaboration.

KEYWORDS: solar and atmospheric neutrinos, neutrino and gamma astronomy, neutrino physics.

Contents

1. Introduction	1
2. Global oscillation solutions	3
2.1 Three strategies	4
2.2 Allowed and disfavored solutions	6
2.3 Allowed ranges of mass, mixing angle, and ${}^8\text{B}$ neutrino flux	8
2.4 The Predicted Energy and Day-Night Dependence	9
2.5 Analysis details for aficionados	11
3. Global “Before and After”	12
4. Predictions for SNO, BOREXINO, and KamLAND	13
4.1 Predictions for MSW solutions	14
4.2 Predictions for vacuum solutions	17
5. Discussion and summary	17

1. Introduction

The goal of this paper is to assess the impact of recent SNO measurements [1, 2, 3] on the allowed regions of neutrino oscillation parameters and on the predicted values of future solar neutrino observables. The SNO collaboration has reported a neutral current (NC) measurement of the active ${}^8\text{B}$ solar neutrino flux and related measurements of the day-night asymmetry, as well as improved determinations of the charged current (CC) and neutrino-electron scattering rate.

We begin in section 2 by deriving the currently allowed regions in neutrino oscillation space using three different analysis strategies (see figure 1), each strategy previously advocated by a different set of authors. The global solutions obtained here are calculated using the methods described in our recent paper [4] (see especially section 3.3 of ref. [4]) but also include some refinements in addition to the new SNO data. For example, we take account of the energy dependence and correlations of the errors in the neutrino absorption cross sections for the chlorine and gallium solar neutrino experiments as described in the Appendix of ref. [5]. We also include

the recently reported SAGE [6] data for 11 years of observation and the zenith angle-recoil energy spectrum data presented by the Super-Kamiokande collaboration after 1496 days of observations [7]. Where required, we use the predicted fluxes and their errors from the BP00 standard solar model [8].

We present in section 3, and especially in figure 3, a “Before and After” comparison of the globally allowed neutrino oscillation solutions (see figure 3). In the “Before” case, we use all the solar neutrino data (see refs. [9, 10, 11, 12, 13, 14, 15]) that were published or had appeared publicly before June 20, 2002, the date that the SNO NC and day-night asymmetry were first published. In the “After” case, we include in addition measurements reported in the two recent papers [1, 2] by the Sudbury Neutrino Observatory (SNO) collaboration.

We use in section 4 the allowed regions in neutrino parameter space to predict in table 2 the expected range of the most promising quantities that can be measured accurately in the BOREXINO [16] and KamLAND [17] ^7Be solar neutrino experiments and in the KamLAND reactor experiment, as well as the spectrum distortion and the day-night asymmetry in the SNO CC measurements. To assess the robustness of the predictions, we compare the values predicted using the “After April 20, 2002” global solution (table 2) with the values predicted using the “Before April 20, 2002” solution (table 3).

We summarize and discuss our conclusions in section 5¹.

We do not discuss in this paper the implications of the agreement between the measured [1] flux of active ^8B solar neutrinos and the predicted [8] standard solar model ^8B neutrino flux. The agreement is accidentally too good to be true [see eq. (2.6)]. As more measurements are made of the neutrino flux and of the solar model parameters the agreement should become less precise. We are aware of several recent and ongoing measurements, which are currently not in good agreement, for the low energy cross section factor S_{17} , to which the calculated standard solar model ^8B neutrino flux is proportional. Until the new laboratory measurements of S_{17} converge to a better defined range, we continue to use the standard value adopted in BP00².

¹Several papers [18, 19, 20] have appeared essentially contemporaneously with the present paper and treat some of the same topics with somewhat similar results, although refs. [18, 19, 20] have not calculated predictions for the eight future solar neutrino observables studied in the present paper. On a technical level, as far as we can tell, these papers have not included the potential effect of distortions on the interpretation of the SNO data in terms of individual rates (see section 2.5) nor the correlations and energy dependences of the neutrino absorption cross sections for the chlorine and gallium experiments (see the Appendix of ref. [5]). Both of these effects are included in the present paper. A concise but insightful and informative discussion of the effects of the recent SNO measurements on solar neutrino oscillations is given in the original SNO NC paper [1]. The interested reader may wish to consult in addition a number of recent papers, refs. [21, 22, 23, 24, 25, 26], that have determined from a variety of perspectives the allowed solar neutrino oscillation solutions following the June, 2001 announcement of the SNO CC measurement [9].

²For an insightful discussion of the predicted and measured total ^8B neutrino flux, see ref. [18].

2. Global oscillation solutions

We describe in section 2.1 the oscillation solutions that are allowed with three different analysis prescriptions (see figure 1). We have at different times used all three of the analysis strategies and various colleagues have advocated strongly one or the other of the strategies described here. Given the recent SNO NC measurement, we now prefer the strategy in which the ${}^8\text{B}$ neutrino flux is treated as a free parameter. This strategy is implemented in figure 1a (see the discussion below). A comparison of the results obtained using the three strategies allows one to test the robustness of any conclusion to the method of analysis.

We present in table 1 and section 2.2 the best-fit oscillation parameters for the allowed and the disfavored solutions, treating the ${}^8\text{B}$ neutrino flux as a free parameter. We discuss in this section the C.L. at which different oscillation solutions are acceptable.

In section 2.3, we present and discuss the allowed ranges for Δm^2 , $\tan^2 \theta$, and the total active flux of ${}^8\text{B}$ solar neutrinos.

The SNO experiment detects CC, NC, ES ($\nu - e$ scattering), and background events. The rates from these different processes are correlated because they are, with the present data, observed most accurately in a mode in which all of the events are considered together and a simultaneous solution is made for each of the separate processes using their known angular dependences (with respect to the solar direction) and their radial dependences in the detector, as well as information from direct measurements of the background [1, 2, 3]. Details of how this analysis is done are given in refs. [2, 3].

Since the different processes are coupled together in the analysis, the inferred values for the measured fluxes in each of the CC, NC, and ES modes depend upon the assumed distortion of the CC and ES recoil energy spectra, which in turn depend upon the assumed Δm^2 and $\tan^2 \theta$. In order to avoid this cycle, the SNO collaboration presented [2] results for the CC, NC, and ES fluxes that were determined by assuming that the CC and ES recoil energy spectra are undistorted by neutrino oscillations or any other new physics.

The fluxes inferred using the hypothesis of undistorted energy spectra has been used by refs. [18, 19, 20] in their analyses of the SNO data. This approximation is excellent for the LMA and LOW solutions, as we shall show later in this section (see, e.g., results quoted in section 2.2), because for these solutions the expected distortions are indeed small. The approximation is less accurate for other solutions in which the distortions are more significant.

We have taken account of the energy dependence of the distortion for each value of Δm^2 and $\tan^2 \theta$ using data provided by the SNO collaboration [3]. We describe how we have carried out the details of this analysis in section 2.5.

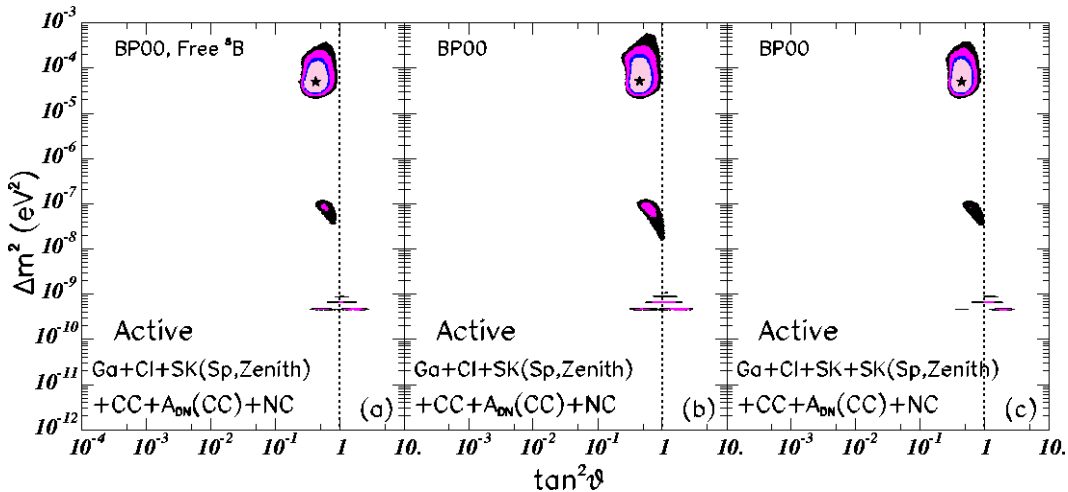


Figure 1: Global neutrino oscillation solutions for three different analysis strategies. The strategy used in constructing panel (a) treats the ${}^8\text{B}$ solar neutrino flux as a free parameter to be determined by the experimental data together with Δm^2 and $\tan^2 \theta$. The strategies corresponding to panels (b) and (c) include the theoretical uncertainty in the ${}^8\text{B}$ neutrino flux, but differ in how they treat the total rate measured in the Super-Kamiokande experiment. The input data used in constructing figure 1 include the neutrino fluxes and uncertainties predicted by the BP00 solar model [8] and the total measured CC and NC event rates from the SNO experiment [1], the SNO day-night asymmetry [2], the Chlorine [10] and Gallium (averaged) [6, 11, 12, 13] event rates, as well as the zenith angle-recoil energy spectrum data presented by Super-Kamiokande [14]. The rates from the GALLEX/GNO and SAGE experiments have been averaged to provide a unique data point (72.4 ± 4.7 SNU). The C.L. contours shown in the figure are 90%, 95%, 99%, and 99.73% (3σ). The global best-fit points are marked by a star.

2.1 Three strategies

Figure 1 shows the allowed ranges of the neutrino oscillation parameters, Δm^2 and $\tan^2 \theta$, that were computed using the three different analysis approaches that have been used previously in the literature. We use the analysis methods and procedures described in refs. [4, 5, 27, 28, 29, 21, 30]), see especially section 3.3 of ref. [4] and the Appendix of ref. [5]. We follow refs. [31, 32] in using $\tan^2 \theta$ (rather than $\sin^2 2\theta$) in order to display conveniently the solutions on both sides of $\theta = \pi/4$.

Figure 1a presents the result for our standard analysis, (a), the free ${}^8\text{B}$ analysis. The strategy used in this standard analysis takes account of the BP00 predicted fluxes and uncertainties for all neutrino sources except for ${}^8\text{B}$ neutrinos. The normalization of the ${}^8\text{B}$ neutrino flux is treated as a free parameter for analysis strategy (a) but is constrained by the BP00 prediction and error for strategies (b) and (c). Analysis strategy (a) considers all the experimental data except for the Super-Kamiokande total event rate. The recoil electron zenith angle-recoil energy spectrum data represent

the Super-Kamiokande total rate in this approach.

Figure 1b displays the results of a calculation, analysis strategy (b), which is the same as for the standard case, figure 1a, except that the ${}^8\text{B}$ neutrino flux is constrained by the BP00 solar model prediction. Prior to the SNO measurement of the NC flux [1], (b) was our standard analysis strategy (cf. ref. [4]). Following the SNO NC measurement, we prefer to use the neutrino data to determine the flux normalization and therefore to test, rather than assume, the standard solar model prediction for the ${}^8\text{B}$ neutrino flux.

Figure 1c was constructed by an analysis similar to that used to construct figure 1b except that for figure 1b the total Super-Kamiokande rate is included explicitly together with a free normalization factor for the zenith angle-recoil energy spectrum of the recoil electrons. This procedure has been used especially effectively by the Bari group [23]³

In all cases, we have accounted for the energy and time dependence of the Super-Kamiokande data by using their zenith angle-recoil energy spectrum data. The available Super-Kamiokande zenith angle-recoil energy spectrum consists of 44 data points, corresponding to six night bins and one day bin for six energy bins between 5.5 and 16 MeV electron recoil energy, plus two daily averaged points for the lowest ($5.0 < E < 5.5$ MeV) and the highest ($E > 16$ MeV) energy bins. Alternatively, one could use their day-night energy spectra as given in 19 energy bins each for the day and for the night periods. Using the more complete zenith angle-recoil energy spectrum data allows for a better discrimination between the LMA and the LOW solutions. Within the LMA regime, oscillations in the Earth are rapid and therefore LMA predicts a rather flat distribution in zenith angle. On the other hand, LOW corresponds to the matter dominated regime of oscillations in the Earth and LOW predicts a well defined structure of peaks in the zenith distribution [33, 34]. The non-observation of such peaks in the zenith angle-recoil energy spectrum data decreases the likelihood of the upper part of the LOW solution as compared to the LMA solution. If one were to use instead the day-night spectra with only night average data, this feature would be missed.

The main difference in the allowed regions shown in the three panels of figure 1 is that strategy (b) allows a slightly larger region for the LOW solution. For the marginally-allowed (or disallowed) LOW region, the required value for the ${}^8\text{B}$ neutrino flux can be significantly different from the standard solar model or the SNO NC value (the two are virtually indistinguishable). Thus the inclusion of the standard solar model uncertainty for the ${}^8\text{B}$ neutrino flux increases the error used in computing the χ^2 for this strategy, which has the effect of enlarging the allowed region.

In constructing figure 1, we assumed that only active neutrinos exist. We derive

³The strategies (a), (b), and (c) described here correspond, respectively, to the strategies (c), (a), and (b) discussed in detail in ref. [4].

Solution	Δm^2	$\tan^2(\theta)$	$f_{B,\text{best}}$	χ^2_{\min}	g.o.f.
LMA	5.0×10^{-5}	4.2×10^{-1}	1.07	45.5	49%
LOW	7.9×10^{-8}	6.1×10^{-1}	0.91	54.3	19%
VAC	4.6×10^{-10}	1.8×10^0	0.77	52.0	25%
SMA	5.0×10^{-6}	1.5×10^{-3}	0.89	62.7	5.1%
Just So ²	5.8×10^{-12}	1.0×10^0	0.46	86.3	$\sim 0\%$
Sterile VAC	4.6×10^{-10}	2.3×10^0	0.81	81.6	$\sim 0\%$
Sterile Just So ²	5.8×10^{-12}	1.0×10^0	0.46	87.1	$\sim 0\%$
Sterile SMA	3.7×10^{-6}	4.7×10^{-4}	0.55	89.3	$\sim 0\%$

Table 1: Best-fit global oscillation parameters with all solar neutrino data.

The table gives for the the best-fit values for Δm^2 , $\tan^2 \theta$, χ^2_{\min} , and g.o.f. for all the oscillation solutions among active solar neutrinos that have been previously discussed (see, e.g., ref. [21]). The quantity f_B measures the ${}^8\text{B}$ solar neutrino flux in units of the predicted BP00 neutrino flux, see eq. (2.5). The oscillation solutions are obtained by varying the ${}^8\text{B}$ flux as free parameter in a consistent way: simultaneously in the rates and in the night and day spectrum fits. The differences of the squared masses are given in eV². The number of degrees of freedom is is 46 [44 (zenith spectrum) + 4 (rates) + 1 ($A_{DN}(CC)$) − 3 (parameters: Δm^2 , θ , and f_B)]. The goodness-of-fit given in the last column is calculated relative to the minimum for each solution. (Solutions that have $\chi^2_{\min} \geq 45.2 + 11.8 = 57.0$ are not allowed at the 3σ C.L.)

therefore the allowed regions in χ^2 using only two free parameters: Δm^2 and $\tan^2 \theta$ ⁴. We use the standard least-square analysis approximation for the definition of the allowed regions with a given confidence level. As shown in ref. [25] the allowed regions obtained in this way are very similar to those obtained by a Bayesian analysis.

2.2 Allowed and disfavored solutions

Table 1 gives for our standard analysis strategy (cf. figure 1a) the best-fit values for Δm^2 and $\tan^2 \theta$ for all the neutrino oscillation solutions that were discussed in our previous analysis in ref. [21]. The table also lists the values of χ^2_{\min} for each solution. The regions for which the local value of χ^2_{\min} exceeds the global minimum by more than 11.83 are not allowed at 3σ C.L.

Within the MSW regime, only the LMA and LOW solutions are allowed at 3σ with the currently available data. The difference in $\Delta\chi^2$ between the global best-fit

⁴The allowed regions for a given C.L. are defined in this paper as the set of points satisfying the condition

$$\chi^2(\Delta m^2, \theta) - \chi^2_{\min} \leq \Delta\chi^2(\text{C.L., 2 d.o.f.}),$$

with $\Delta\chi^2(\text{C.L., 2 d.o.f.}) = 4.61, 5.99, 9.21$, and 11.83 for C.L. = 90%, 95%, 99% and 99.73% (3σ)

point (in the LMA allowed region) and the best-fit LOW point is $\Delta\chi^2 = 8.8$, which implies that the LOW solution is allowed only at the 98.8% C.L. (2.5σ).

The vacuum solution is currently allowed at the 96% C.L. (2.1σ). This solution is also allowed in our Before analysis, which we present later in figure 3, at a C.L. better than 95% C.L. (and also in the most recent Super-Kamiokande analysis [7]). But it was not found by the SNO collaboration at the 3σ level. This difference may be due to the careful use by the SNO collaboration of the full information regarding the recoil energy spectrum, or to our more complete treatment of the theoretical errors, or to some more subtle difference in the analysis procedures (such as a too-sparse grid in Δm^2). Whatever the reason, the vacuum solution is not robustly present. If we use the neutrino fluxes determined by SNO assuming that the recoil energy spectrum is undistorted and neglect the statistical correlations, the vacuum solutions are not allowed at 3.1σ .

For oscillation solutions for which the survival probability does not depend strongly upon energy, such as the LMA and LOW solutions, the effects of including [2, 3] the energy distortion in the determination of the rates is very small. We find, using the procedure described in section 2.5, that the central values of the CC and NC fitted rates for the best fit points in LMA (LOW) in table 1 are shifted by $+0.5\%$ and -1.5% (0% and $+3\%$), respectively, with respect to the values obtained under the hypothesis of no energy distortion. This results in an increase of the $\Delta\chi^2$ between LMA and LOW of ~ 0.2 (i.e., by about 2%). For solutions with stronger energy dependences such as SMA (VAC), the effects are larger and lead to shifts in the central values of the CC and NC rates of -1.5% and $+15.5\%$ ($+10\%$ and -11%).

We have made a number of checks on the stability of our conclusions regarding the global solutions. The $\Delta\chi^2$ between LMA and LOW is rather robust under small changes in the method of error treatment and in the fitting procedure. However, the C.L. at which the VAC and the QVO solutions (the region between the LOW solutions and the VAC solutions, see the insightful discussion by Friedland [35]) are allowed may fluctuate from just below to just above the 3σ limit, depending upon details of the analysis. For example, all VAC solutions are disfavored at 3σ if one ignores the anti-correlation between the statistical errors of the NC and the CC rates.

The best-fitting pure sterile solution is VAC, which is excluded at 5.4σ C.L. (for 3d.o.f.). Before April 20, 2002, the best-fitting pure sterile solution was SMA sterile, which was acceptable at 3.6σ .

Oscillations into an admixture of active and sterile neutrinos are still possible as long as the assumed total ${}^8\text{B}$ neutrino flux is increased appropriately [5, 18]. This uncertainty can be reduced by combining SNO solar neutrino data with results from the terrestrial KamLAND reactor experiment [5].

Our value for $\Delta\chi^2 = \chi^2_{\text{LOW}} - \chi^2_{\text{LMA}}$ may be lower than most other groups who do similar calculations because we include the effect of the correlations and the energy dependence of the neutrino absorption cross sections for the gallium and chlorine

solar neutrino experiments (see the Appendix of ref. [5]). The cross section effects correspond to $\Delta\chi^2 = -1.3$ for the current global allowed solution, strategy (a). Taking this effect into account, our values for $\Delta\chi^2$ between the LMA and LOW solutions seems to be in general agreement with most other authors [1, 19, 20], although there is a rather significant difference between our result of $\Delta\chi^2 = 8.8$ and the result given by Barger et al. in ref. [18] ($\Delta\chi^2 = 4.7$)⁵.

2.3 Allowed ranges of mass, mixing angle, and ${}^8\text{B}$ neutrino flux

The upper limit on the allowed value of Δm^2 is important for neutrino oscillation experiments, as stressed in ref. [22]. In units of eV², we find for the LMA solution the following 3σ limits on Δm^2

$$2.3 \times 10^{-5} < \Delta m^2 < 3.7 \times 10^{-4}. \quad (2.1)$$

The LMA solar neutrino region does not reach the upper bound for Δm^2 imposed by the CHOOZ reactor data [15], i.e., $\Delta m^2 \leq 8 \times 10^{-4}$ eV². Prior to April 20, 2002, the solar neutrino data alone were not sufficient to exclude LMA masses above the Chooz bound.

For the LOW solution only the following small mass range is allowed,

$$3.5 \times 10^{-8} < \Delta m^2 < 1.2 \times 10^{-7}. \quad (2.2)$$

Many authors (see, e.g., ref. [36] and references quoted therein) have discussed the possibility of bi-maximal neutrino oscillations, which in the present context implies $\tan^2 \theta = 1$. Figure 1 shows that precise bi-maximal mixing is disfavored for both the LMA and LOW solutions. Quantitatively, we find that there are no solutions with $\tan^2 \theta = 1$ at the 3.3σ C.L. for the LMA solution, at the 3.2σ C.L. for the LOW solution, and at the 2.8σ C.L. for the VAC solutions. These results refer to our standard analysis strategy, corresponding to panel (a) of figure 1.

Of course, approximate bi-maximal mixing is now heavily favored. Atmospheric neutrinos oscillate with a large mixing angle [37] and all the currently allowed solar oscillations correspond to large mixing angles (see figure 1).

How close are the solar neutrino mixing angles to $\pi/4$? At three sigma, we find the following allowed range for the LMA mixing angle

$$0.24 < \tan^2 \theta < 0.89, \quad (2.3)$$

and for the LOW solution

$$0.43 < \tan^2 \theta < 0.86. \quad (2.4)$$

⁵They find that the LOW solution is allowed at 90% C.L. [18], whereas we find it is only allowed at 99% C.L. Barger et al. use the day-night spectrum instead of the zenith angle-recoil energy spectrum used here. As discussed above, the zenith angle-recoil energy spectrum allows a better discrimination between the LOW and LMA solutions. Despite these technical differences, their best-fit LMA point is essentially identical with the one found here.

Let f_B be the ${}^8\text{B}$ neutrino flux inferred from global fits to all the available solar neutrino data. Moreover, let f_B be measured in units of the best-estimate predicted BP00 neutrino flux ($5.05 \times 10^6 \text{ cm}^{-2}\text{s}^{-1}$),

$$f_B = \frac{\phi({}^8\text{B})}{\phi({}^8\text{B})_{\text{BP00}}}. \quad (2.5)$$

The best-fit values for f_B for each of the oscillation solutions are listed in the fourth column of table 1.

The value of f_B found by the SNO collaboration from their neutral current measurement via a simultaneous solution for all reactions in the SNO detector is [1]

$$f_B = 1.01[1 \pm 0.12] \text{ (1}\sigma\text{).} \quad (2.6)$$

For the global solution shown in figure 1a, the $1\sigma[3\sigma]$ allowed range of f_B in the LMA solution region is

$$f_B = 1.07 \pm 0.08 \text{ (1}\sigma\text{)} \quad [f_B = 1.07^{+0.23}_{-0.25} \text{ (3}\sigma\text{)} \text{ (LMA).} \quad (2.7)$$

The 3σ range of f_B in the LOW solution region is

$$f_B = 0.91^{+0.03}_{-0.02} \text{ (3}\sigma, \text{ LOW).} \quad (2.8)$$

For both eq. (2.7) and eq. (2.8), the range of f_B was calculated by marginalizing over the full space of oscillation parameters (Δm^2 , $\tan^2 2\theta$) using the global minimum value for χ^2 which lies in the LMA allowed region.

The allowed range of the ${}^8\text{B}$ active solar neutrino flux derived from the global oscillation solution and given in eq. (2.7) is slightly more restrictive than was found by the SNO collaboration using just their NC measurement (cf. eq. 2.6).

2.4 The Predicted Energy and Day-Night Dependence

Figure 2 shows the predicted energy dependence and the day-night asymmetry for the survival probability $P(\nu_e \rightarrow \nu_e)$ of the allowed MSW oscillation solutions, the LMA and LOW solutions, as well as the best-fit vacuum solution.

We plot in figure 2 the best-fit survival probabilities for an electron neutrino that is created in the Sun to remain an electron neutrino upon arrival at a terrestrial detector. The right-hand panels present the survival probability for energies between 0 and 15 MeV. The left-hand panels present blow-ups of the behavior of the solutions at energies less than 1 MeV.

The energy dependence of both MSW solutions is predicted to be very modest above 5 MeV, in agreement with the fact that no statistically significant distortion of the recoil energy spectrum has yet been observed in the Super-Kamiokande experiment [14]. For the SNO CC measurements, table 2 shows that the expected

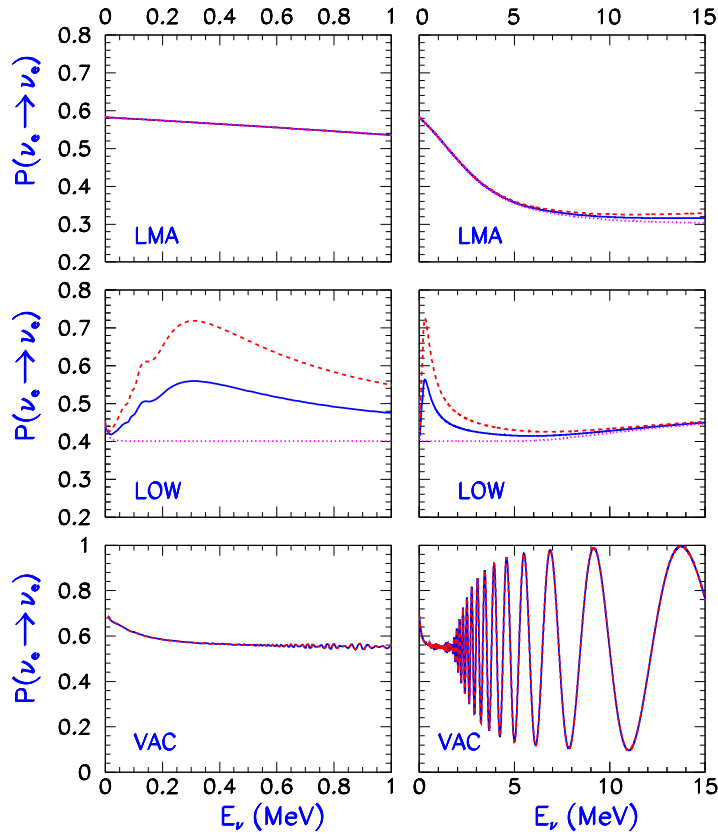


Figure 2: Survival Probabilities. The figure presents the yearly-averaged best-fit survival probabilities determined with strategy (a) for an electron type neutrino that is created in the center of the Sun and arrives at a detector on Earth. The full line refers to the average survival probabilities computed taking into account regeneration in the Earth and the dotted line refers to calculations for the daytime that do not include earth regeneration. The dashed line include regeneration at night. The regeneration effects are computed for the location of the SNO detector for the right hand panels and for the location of the Gran Sasso Underground Laboratory for the left hand panels. There are only slight differences between the computed regeneration effects for detectors located at the positions of SNO, Super-Kamiokande, and Gran Sasso (see ref. [38]) The LOW solutions in the right-hand panel are averaged over a small energy band, 0.1 MeV, to suppress rapid oscillations caused by a sensitive dependence upon the Earth-Sun distance. The vacuum solutions are averaged over an energy band of ± 0.05 MeV.

distortions of the first and second moments of the electron recoil energy spectrum are predicted to be too small to be measurable with statistical significance.

At energies below 5 MeV, both the LMA and the LOW solutions are predicted to exhibit a significant energy dependence.

At the energies at which water Cherenkov experiments have been possible, the

survival probability $P(\nu_e \rightarrow \nu_e) \approx 1/3$, i.e., approximately one over the number of known neutrinos. According to MSW theory, this is an accident. We see from figure 2 that a survival probability of order 0.5 is predicted for energies less than 1 MeV.

The day-night asymmetry is potentially detectable for the LMA solution only at energies above 5 MeV; the predicted asymmetry increases with energy (see figure 2). The situation is just the opposite for the LOW solution. The day-night asymmetry is large below 5 MeV and relatively small above 5 MeV.

The vacuum solution has rapid oscillations in energy above 2 MeV (see figure 2), but these oscillations would be very difficult to observe because they tend to average out over a typical experimental energy bin. At lower energies, the vacuum oscillations will also appear to be smooth, again because of the difficult of resolving in energy the oscillations. There should be no measurable day-night asymmetry if the vacuum oscillation solution is correct.

2.5 Analysis details for aficionados

The relatively precise values of the CC and NC rates given in the recent SNO paper [1] were extracted by a fit to the observed recoil energy spectrum using the assumption of an undistorted spectrum, *i.e.* for a survival probability that is constant in time⁶. These rates cannot be used directly to test an oscillation hypothesis which would cause significant distortions of the CC and ES recoil energy spectra. Since they were aware of the inconsistency in doing so, the SNO collaboration did not use in their oscillation analysis the rates extracted assuming undistorted spectra. Instead, they correctly performed a direct fit to their summed spectrum, including the three contributions from NC, CC and ES (as well as the background) computed for each point in oscillation parameter space.

We include the spectral distortions in a somewhat different way than was done by the SNO collaboration. We perform a two step analysis, which has-as we shall see-advantages and disadvantages. We use the data generously provided by the SNO collaboration [3].

- First, for a given point in oscillation parameter space, we compute the expected distortions of the CC and ES recoil energy spectra, and then add these spectra to the NC energy spectrum (which, with a little thought, one can see is undistorted for either active or sterile oscillations). We fit the summed SNO energy spectrum to obtain the shifts in the normalization of the NC and CC rates (shifts with respect to the values obtained for undistorted energy spectra). Thus, we obtain as a function of the oscillation parameters, the best-fit

⁶They also quote the NC rate obtained from a fit with arbitrary distortion, which results into a much less precise determination.

CC and NC measured rates (and their corresponding statistical errors, which are strongly anti-correlated).

- Second, with these NC and CC rates, we compute the χ^2 for each particular point in oscillation space, combining these two measurements with the available results of all other solar neutrino experiments. We use the three different analysis strategies discussed in ref. [4] and in section 2.1 of this paper. We use for the SNO day-night asymmetry the result quoted for an undistorted spectrum [2], since the small effect of the distortion is expected to nearly cancel out in the asymmetry. In combining the NC and CC data, we take account of the correlation between their errors (both statistical and systematic). We make the excellent approximation that the systematic uncertainties have the same percentage values [1, 2] as they have for the undistorted rates.

With this two-step procedure and the data provided by the SNO collaboration [3], we can rather quickly take into account the effects of the distortions due to neutrino oscillations of the CC and ES recoil energy spectrum. Moreover, we can monitor and understand the main effects of the distortions on the extracted CC and NC rates. This allows us to check our code in a variety of different ways. However, we do not use the full power of the spectral energy information that is known to the SNO collaboration.

Given that the spectral energy distortions are strongly constrained by the fact that Super-Kamiokande [7, 14] does not observe a significant distortion, we think it is unlikely that the two methods of taking account of distortions—the one used by the SNO collaboration and the one used here—will lead to significantly different results when analyzing actual solar neutrino experimental data.

3. Global “Before and After”

What is the impact of the recent SNO measurements [1, 2] on the globally allowed regions of neutrino oscillation parameters?

Figure 3 compares the allowed regions that are found with the solar neutrino data available prior to the presentation of the recent SNO data (i.e., prior to April 20, 2002) with the allowed regions found including the recent SNO data [1, 2]. We like to refer to figure 3 as our “Before and After” figure.

The left panel of figure 3 was computed including the improvements that we described in section 1 regarding the neutrino cross section errors and correlations and the improved average gallium event rate. Hence figure 3a does not correspond to any previously published global oscillation solution, although it could have been computed prior to April 20, 2002.

The recent SNO measurements have greatly shrunk the allowed region for the LOW solution and have significantly reduced the allowed region for the LMA solution,

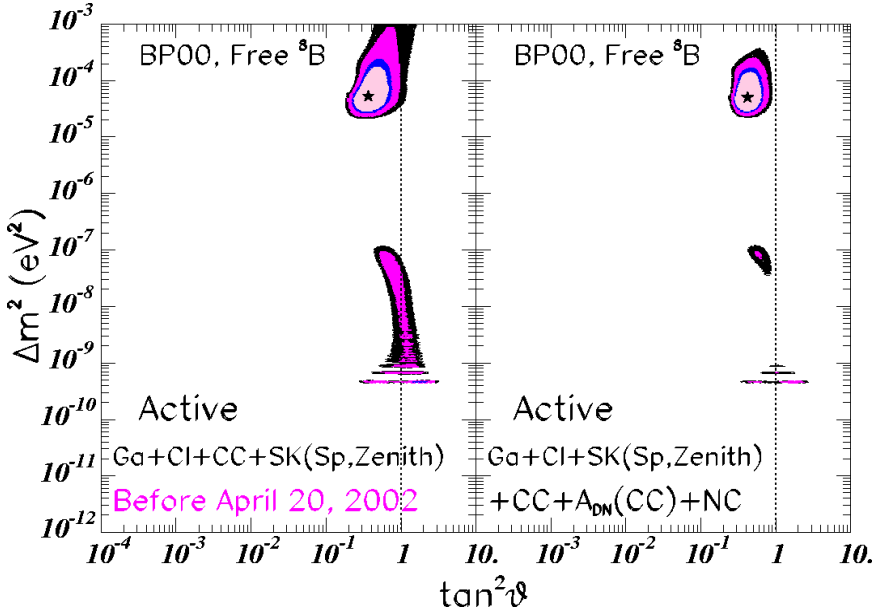


Figure 3: Global “Before and After.” The left panel shows the allowed regions for neutrino oscillations computed using solar neutrino experimental data available prior to June 20 2002. The right panel shows the allowed region computed with the same procedure but including the SNO NC and improved CC data [1] and the SNO day-night asymmetry [2]. In the “Before” panel, the LOW solution is allowed at 97.4% and in the “After” panel LOW is allowed at the 98.8%.

as can be seen by comparing the two panels of figure 3. In particular, maximal mixing is now not allowed at 3σ and the region does not reach the Chooz reactor bound, $\Delta m^2 \leq 8 \times 10^{-4} \text{ eV}^2$ [15].

The LOW solution is now allowed at the 98.8% C.L. Before the recent SNO measurements, the LOW solution was allowed at 97.4%.

4. Predictions for SNO, BOREXINO, and KamLAND

We summarize in this section some of the most important predictions that follow from the global neutrino oscillation solutions discussed in section 1 and section 3. To test the robustness of the predictions given in this section, we have calculated the expected values and allowed ranges by two different methods: 1) using the precise values for the CC and NC given in ref. [1] assuming no spectral energy distortions and 2) taking account of the potential effects of spectral energy distortions on the SNO measurements as described in section 2.5. The differences in the calculated values and ranges are negligible in all cases. We present here, for consistency with figure 1 and our previous discussion, the values calculated taking account of the potential spectral distortions in the SNO data.

Observable	b.f. $\pm 1\sigma$	LMA $\pm 3\sigma$	LOW $\pm 3\sigma$
A_{N-D} (SNO CC) (%)	$4.7^{+3.4}_{-3.2}$	$4.7^{+9.1}_{-4.7}$	$2.7^{+2.7}_{-2.1}$
δT (SNO CC) (%)	$-0.17^{+0.19}_{-0.56}$	$-0.17^{+0.31}_{-1.55}$	$0.42^{+0.55}_{-0.35}$
$\delta\sigma$ (SNO CC) (%)	$0.03^{+0.17}_{-0.61}$	$0.03^{+0.25}_{-1.77}$	$0.42^{+0.55}_{-0.35}$
[R (^7Be)]	0.64 ± 0.03	$0.64^{+0.09}_{-0.05}$	0.58 ± 0.05
A_{N-D} (^7Be) (%)	$0.0^{+0.0}_{-0.0}$	$0.0^{+0.1}_{-0.0}$	23^{+10}_{-13}
[CC] (KamLAND)			
$(E_{\text{th}} = 2.72 \text{ MeV})$	$0.49^{+0.20}_{-0.17}$	$0.49^{+0.25}_{-0.26}$	—
$(E_{\text{th}} = 1.22 \text{ MeV})$	0.52 ± 0.15	$0.52^{+0.20}_{-0.25}$	—
$\delta E_{\text{visible}}$ (KamLAND) (%)			
$(E_{\text{th}} = 2.72 \text{ MeV})$	-7^{+13}_{-2}	-7^{+14}_{-4}	—
$(E_{\text{th}} = 1.22 \text{ MeV})$	-9^{+13}_{-3}	-9^{+17}_{-5}	—
$\delta\sigma$ (KamLAND) (%)			
$(E_{\text{th}} = 2.72 \text{ MeV})$	-5^{+11}_{-10}	-5^{+20}_{-14}	—
$(E_{\text{th}} = 1.22 \text{ MeV})$	-8^{+20}_{-8}	-8^{+26}_{-12}	—

Table 2: “After” Predictions. This table presents for future solar neutrino observables the best-fit predictions and 1σ and 3σ ranges that were obtained by using analysis strategy (a) and all solar neutrino data currently available. The best-fit values and uncertainties given here correspond to the allowed regions in the right hand panel of figure 3; i.e., this table was constructed by including the data made available by the SNO collaboration on April 20, 2002 [1, 2]. The day-night asymmetries for the SNO and the ^7Be (BOREXINO) experiments are denoted by A_{N-D} and are defined by eq. (4.1). The reduced ^7Be event rate is defined by eq. (4.2); the reduced KamLAND CC rate is defined by eq. (4.3). The first moment of the recoil electron energy distribution is denoted by δT for SNO and $\delta E_{\text{visible}}$ for KamLAND; the second moments are denoted by $\delta\sigma$. The threshold of the recoil electron kinetic energy used in computing the SNO observables for this table is 5 MeV. For the BOREXINO experiment, we consider electron recoil energies between between 0.25 MeV and 0.8 MeV (see ref. [16]). We present the results for the KamLAND reactor observables for two thresholds, $E_{\text{th}} = 1.22$ and 2.72 MeV.

We summarize in section 4.1 the predictions for the MSW solutions. We answer the following question in section 4.2: How can we distinguish between vacuum and MSW solutions?

4.1 Predictions for MSW solutions

Table 2 presents the best-fit predictions and the expected ranges for eight important future solar neutrino observables. The results summarized in table 2 correspond to

the right-hand side (the “After” panel) of figure 3. The notation used here is the same as in ref. [4].

How much of a difference have the recent SNO measurements made in the expected values for future solar neutrino observables? The reader can answer this question by comparing table 3 with table 2. Here, table 3 presents the best-fit predictions and allowed ranges that correspond to using solar neutrino data available prior to April 20, 20002. In particular, the values given in table 3 were obtained using the global solution shown in the left-hand side, the “Before” panel, of figure 3.

The principal differences between the results summarized in table 2 and table 3 are a consequence of the smaller allowed region of the LOW solution shown in the “After” panel of figure 3. The changes that result from the modest reduction of the LMA allowed region are generally not very significant.

The predicted day-night asymmetries, A_{N-D} , between the nighttime and the daytime event rates for SNO and for BOREXINO (${}^7\text{Be} \nu - e$ scattering detector) are given in the first and third rows, respectively, of table 2 and table 3. The results presented correspond to an average over one year. The definition of A_{N-D} is

$$A_{N-D} = 2 \frac{[\text{Night} - \text{Day}]}{[\text{Night} + \text{Day}]} . \quad (4.1)$$

The minimum predicted value for the day-night asymmetry, A_{N-D} (${}^7\text{Be}$), in BOREXINO is now a whopping-big 12% at 3σ , whereas prior to April 20, 2002, A_{N-D} (${}^7\text{Be}$) equal to 0% was allowed. There are no significant differences in the Before and After predictions for A_{N-D} (SNO CC).

The first and second moments of the SNO CC spectrum for the case of no oscillations are $\langle T_0 \rangle = 7.74\text{MeV}$ and $\langle \sigma_0 \rangle = 1.87\text{ MeV}$. The range of predicted shifts with respect to these no-oscillation values is always smaller than $\sim 2\%$ within both the LMA and LOW 3σ regions and is not significantly different from the range found in the “Before” analysis. Larger shifts for the moment second moment (7%) are possible within the allowed VAC oscillation region. The non-statistical uncertainties in measuring the first and second moments in SNO have been estimated, prior to the operation of the experiment, in ref. [39] and are, respectively, about 1% and 2%.

Based upon the results given in table 2, we predict that SNO will not measure a statistically significant ($> 3\sigma$) distortion to the recoil energy spectrum for the CC reaction. This prediction constitutes an important consistency test of the oscillation analysis and the understanding of systematic effects in the detector.

The prediction for the reduced ${}^7\text{Be} \nu - e$ scattering rate,

$$[{}^7\text{Be}] \equiv \frac{\text{Observed } \nu - e \text{ scattering rate}}{\text{BP00 predicted rate}} , \quad (4.2)$$

is remarkably precise and remarkably stable. The current prediction for what BOREXINO will measure if the LMA solution is valid is $[{}^7\text{Be}] = 0.64^{+0.04}_{-0.03}$. A somewhat smaller value is predicted if the LOW solution is correct.

Observable	b.f. $\pm 1\sigma$	LMA $\pm 3\sigma$	LOW $\pm 3\sigma$
A_{N-D} (SNO CC) (%)	$4.4^{+3.9}_{-3.1}$	$4.4^{+11.4}_{-4.4}$	$1.3^{+3.9}_{-1.3}$
δT (SNO CC) (%)	$-0.23^{+0.25}_{-0.57}$	$-0.23^{+0.39}_{-1.58}$	$0.25^{+0.71}_{-0.44}$
$\delta\sigma$ (SNO CC) (%)	$0.16^{+0.12}_{-0.78}$	$0.16^{+0.13}_{-2.0}$	$0.25^{+0.96}_{-1.02}$
[R (^7Be)]	0.66 ± 0.04	$0.66^{+0.09}_{-0.07}$	$0.59^{+0.13}_{-0.06}$
A_{N-D} (^7Be) (%)	—	$0.0^{+0.1}_{-0.0}$	15^{+17}_{-15}
[CC] (KamLAND)			
$(E_{\text{th}} = 2.72 \text{ MeV})$	$0.56^{+0.14}_{-0.22}$	$0.56^{+0.20}_{-0.34}$	—
$(E_{\text{th}} = 1.22 \text{ MeV})$	$0.57^{+0.1}_{-0.18}$	$0.57^{+0.16}_{-0.31}$	—
$\delta E_{\text{visible}}$ (KamLAND) (%)			
$(E_{\text{th}} = 2.72 \text{ MeV})$	-7^{+12}_{-2}	-7^{+14}_{-4}	—
$(E_{\text{th}} = 1.22 \text{ MeV})$	-7^{+11}_{-4}	-7^{+15}_{-7}	—
$\delta\sigma$ (KamLAND) (%)			
$(E_{\text{th}} = 2.72 \text{ MeV})$	-6^{+16}_{-9}	-6^{+21}_{-12}	—
$(E_{\text{th}} = 1.22 \text{ MeV})$	-9^{+19}_{-7}	-9^{+28}_{-11}	—

Table 3: “Before” Predictions. This table presents for future solar neutrino observables the best-fit predictions and 1σ and 3σ ranges that were obtained by using analysis strategy (a) and solar neutrino data available before April 20, 2002. The best-fit and uncertainties given here correspond to the allowed regions in the left hand panel of figure 3. The format and procedures used in constructing this table are the same as used in constructing table 2 except that here we have not included the recent SNO data [1, 2].

The predicted value of the reduced CC event rate in the KamLAND reactor experiment,

$$[\text{CC}](\text{KamLAND}) \equiv \frac{\text{Observed } \bar{\nu} + p \text{ absorption rate}}{\text{No oscillation rate}} , \quad (4.3)$$

is not significantly affected by the recent SNO results. The best-fit prediction shifts slightly (to a lower value) but the shift is well-within the 1σ currently allowed range.

For KamLAND, it is convenient to represent the distortion of the visible energy spectrum by the fractional deviation from the undistorted spectrum of the first two moments of the energy spectrum. We follow the notation and analysis of refs. [4, 39, 40]. The predicted fractional distortion of the first two moments is not significantly affected by the recent SNO measurements. Since table 2 and table 3 give only the fractional changes of the moments relative to the moments for the undistorted spectrum, we must also specify the values calculated for a spectrum unaffected by new physics. In the absence of oscillations, one expects [4]: $\langle E_{\text{vis}} \rangle_0 = 3.97 \text{ MeV}$ and

$\langle\sigma\rangle_0 = 1.26$ MeV for $E_{\text{threshold}} = 1.22$ MeV ($\langle E_{\text{vis}} \rangle_0 = 4.33$ MeV and $\langle\sigma\rangle_0 = 1.06$ MeV for $E_{\text{threshold}} = 1.72$ MeV).

4.2 Predictions for vacuum solutions

The clearest evidence against the vacuum oscillations would be the observation of a rate depletion or a spectral distortion in the KamLAND reactor experiment. The Δm^2 for vacuum oscillations is too small to lead to an observable effect with KamLAND.

Within the 3σ allowed VAC regions, the distortion of the SNO spectrum corresponds to a shift in the first (second) moment of the recoil energy distribution of at most -2% (+6%) and no significant seasonal variation at SNO is expected. The predicted ${}^7\text{Be}$ rate for vacuum oscillations at BOREXINO is in the same range as the predictions for LMA and LOW solutions. The most striking signal for vacuum oscillations would be the observation of a large seasonal variation in the BOREXINO experiment, with a clear pattern of the monthly dependence of the observed rate [41]. There should also be a day-night effect at BOREXINO associated with this seasonal variation; the day-night asymmetry should be at most $\pm 8\%$ (the size and sign of this asymmetry is sensitive to the exact value of Δm^2 considered to be within the allowed VAC islands) due to the dependence of the survival probability upon the earth-sun distance.

5. Discussion and summary

Figure 1 and figure 3, together with table 1, tell much of the story. These global analyses, which use all the available solar neutrino data, demonstrate that only large mixing angle solutions are currently allowed at the 3.7σ confidence level.

We therefore know at an impressive confidence level that there are relatively large mixing angles for oscillations between solar neutrinos (and between atmospheric neutrinos), unlike the small mixing angles among quarks. However, precise maximal mixing is excluded at 3.2σ for MSW solutions (see eq. 2.3 and eq. 2.4 for the exact allowed regions) and at 2.8σ for vacuum oscillations. The situation with masses and mixing angles for solar neutrinos does not appear to be particularly simple.

Among the MSW solutions, the situation has also been clarified. The LMA solution is now the only viable solution at a level of 2.5σ . The LOW solution is excluded at the 98.8% C.L. The KamLAND and BOREXINO experiments will test strongly this conclusion. The SMA solution is now excluded at more than 3.7σ . Pure sterile oscillations are excluded at 5.4σ .

The global oscillation solutions constrain the active ${}^8\text{B}$ solar neutrino flux with comparable accuracy to the SNO NC measurement [1]. The accuracy of the SNO NC measurement is $\pm 12\%$. We find from a global oscillation solution of all the data, $f_{\text{B}} = 1.07 \pm 0.08(1\sigma)$ (LMA solution), where f_{B} is the total flux of active ${}^8\text{B}$ solar

neutrinos in units of the flux predicted by the standard solar model [8]. The allowed ranges of f_B for the LMA and LOW solutions are given in eq. (2.7) and eq. (2.8), respectively, at 1σ and 3σ C.L.

We have calculated the predicted best-fit values and ranges for eight important solar neutrino observables for the BOREXINO, KamLAND, and SNO experiments. The results are summarized in the “Before” and “After” tables, table 2 and table 3, and in section 4.2. The predictions are relatively robust. Only the predictions for the disfavored LOW solution are significantly affected by the recent SNO measurements [1, 2]. We have calculated the predicted values and ranges given in table 2 and table 3 both with and without taking account of potential spectral energy distortions in interpreting the SNO data (see section 2.5 and ref. [3]). Both methods give essentially identical results.

For the reader who (like us) often prefers pictures to tables, figure 2 shows the predicted energy dependence and day-night difference for the current best-fit LMA and LOW solutions.

We are grateful to the SNO collaboration for the thrill of analyzing solar neutrino data that include a neutral current measurement. JNB acknowledges support from NSF grant No. PHY0070928. MCG-G is supported by the European Union Marie-Curie fellowship HPMF-CT-2000-00516. This work was also supported by the Spanish DGICYT under grants PB98-0693 and FPA2001-3031.

References

- [1] SNO collaboration, Q.R. Ahmad et al., *Direct evidence for neutrino flavor transformation from neutral-current interactions in the Sudbury Neutrino Observatory*, nucl-ex/0204008.
- [2] SNO collaboration, Q.R. Ahmad et al., *Measurement of day and night neutrino energy spectra at SNO and constraints on neutrino mixing parameters*, nucl-ex/0204009.
- [3] <http://www.sno.phy.queensu.ca/>. See discussion entitled “Data from the SNO NC and Day/Night PRLs,” posted 26/04/2002.
- [4] J.N. Bahcall, M.C. Gonzalez-Garcia, and C. Peña-Garay, *Robust signatures of solar neutrino oscillation solutions*, *J. High Energy Phys.* **04** (2002) 007.
- [5] J.N. Bahcall, M.C. Gonzalez-Garcia, and C. Peña-Garay, hep-ph/0204194.
- [6] SAGE collaboration, J.N. Abdurashitov, *Measurement of the solar neutrino capture rate by the Russian-American gallium solar neutrino experiment during one half of the 22-year cycle of solar activity*, astro-ph/0204245.
- [7] M.B. Smy, *A unique oscillation solution to the solar neutrino problem?*, hep-ex/0202020.
- [8] J.N. Bahcall, M.H. Pinsonneault, S. Basu, *Solar models: current epoch and time dependences, neutrinos, and helioseismological properties*, *Astrophys. J.* **555** (2001) 990.
- [9] SNO collaboration, Q.R. Ahmad et al., *Measurement of charged current interactions produced by ${}^8\text{B}$ solar neutrinos at the Sudbury Neutrino Observatory*, *Phys. Rev. Lett.* **87** (2001) 071301.
- [10] B.T. Cleveland et al., *Measurement of the solar electron neutrino flux with the Homestake chlorine detector*, *Astrophys. J.* **496** (1998) 505.
- [11] GALLEX collaboration, W. Hampel et al., *GALLEX solar neutrino observations: results for GALLEX IV*, *Phys. Lett.* **B 447** (1999) 127.
- [12] GNO collaboration, M. Altmann et al., *GNO solar neutrino observations: results for GNO I*, *Phys. Lett.* **B 490** (2000) 16; GNO collaboration, E. Bellotti et al., *First results from GNO*, in *Neutrino 2000*, Proc. of the XIXth International Conference on Neutrino Physics and Astrophysics, 16–21 June 2000, eds. J. Law, R.W. Ollerhead, and J.J. Simpson, *Nucl. Phys.* **B 91** (*Proc. Suppl.*) (2001) 44.
- [13] SAGE collaboration, J.N. Abdurashitov et al., *Measurement of the solar neutrino capture rate with gallium metal*, *Phys. Rev.* **C 60** (1999) 055801 [astro-ph/9907113]; SAGE collaboration, V. Gavrin, *Solar neutrino results from SAGE*, in *Neutrino 2000*, Proc. of the XIXth International Conference on Neutrino Physics and

Astrophysics, 16–21 June 2000, eds. J. Law, R.W. Ollerhead, and J.J. Simpson, *Nucl. Phys. B* **91** (*Proc. Suppl.*) (2001) 36.

- [14] Super-Kamiokande collaboration, Y. Fukuda et al., *Measurements of the solar neutrino flux from Super-Kamiokande's first 300 days*, *Phys. Rev. Lett.* **81** (1998) 1158; Erratum **81** (1998) 4279; *Constraints on neutrino oscillation parameters from the measurement of day-night solar neutrino fluxes at Super-Kamiokande*, *Phys. Rev. Lett.* **82** (1999) 1810; Super-Kamiokande collaboration, Y. Suzuki, *Solar neutrino results from Super-Kamiokande*, in *Neutrino 2000*, Proc. of the XIXth International Conference on Neutrino Physics and Astrophysics, 16–21 June 2000, eds. J. Law, R.W. Ollerhead, and J.J. Simpson, *Nucl. Phys. B* **91** (*Proc. Suppl.*) (2001) 29; Super-Kamiokande collaboration, S. Fukuda et al., *Solar ${}^8\text{B}$ and hep neutrino measurements from 1258 days of Super-Kamiokande data*, *Phys. Rev. Lett.* **86** (2001) 5651.
- [15] M. Apollonio et al., *Limits on neutrino oscillations from the CHOOZ experiment*, *Phys. Lett. B* **466** (1999) 415.
- [16] BOREXINO collaboration, G. Alimonti et al., *Science and technology of BOREXINO: a real time detector for low energy solar neutrinos*, *Astropart. Phys.* **16** (2002) 205.
- [17] KamLAND collaboration, P. Alivisatos et al., *KamLAND: a liquid scintillator anti-neutrino detector at the Kamioka site*, Stanford-HEP-98-03; KamLAND collaboration, A. Piepke, *KamLAND: a reactor neutrino experiment testing the solar neutrino anomaly*, in *Neutrino 2000*, Proc. of the XIXth International Conference on Neutrino Physics and Astrophysics, 16–21 June 2000, eds. J. Law, R.W. Ollerhead, and J.J. Simpson, *Nucl. Phys. B* **91** (*Proc. Suppl.*) (2001) 99.
- [18] V. Barger, D. Marfatia, K. Whisnant, B.P. Wood, *Imprint of SNO neutral current data on the solar neutrino problem*, hep-ph/0204253.
- [19] P. Creminelli, G. Signorelli, A. Strumia, *Frequentist analyses of solar neutrino data*, *J. High Energy Phys.* **05** (2001) 052. See addendum 04/24/2002, hep-ph/0102234.
- [20] A. Bandyopadhyay, S. Choubey, S. Goswami, D.P. Roy, *Implications of the first neutral current data from SNO for Solar Neutrino Oscillation*, hep-ph/0204286.
- [21] J.N. Bahcall, M.C. Gonzalez-Garcia, Carlos Peña-Garay, *Global analysis of solar neutrino oscillations including SNO CC measurement*, *J. High Energy Phys.* **08** (2001) 014.
- [22] P.I. Krastev and A.Yu. Smirnov, *Global analysis with SNO: toward the solution of the solar neutrino problem*, accepted for publication in *Phys. Rev. D* [hep-ph/0108177].

- [23] G.L. Fogli, E. Lisi, D. Montanino, A. Palazzo, *Model-dependent and independent implications of the first Sudbury Neutrino Observatory results*, *Phys. Rev. D* **64** (2001) 093007.
- [24] V. Barger, D. Marfatia, K. Whisnant, *Unknowns after the SNO charged-current measurement*, *Phys. Rev. Lett.* **88** (2002) 011302; V. Barger, D. Marfatia, K. Whisnant, *Piecing the Solar Neutrino Puzzle Together at SNO*, *Phys. Lett. B* **509** (2001) 19.
- [25] M.V. Garzelli and C. Giunti, *Bayesian view of solar neutrino oscillations*, *J. High Energy Phys.* **12** (2001) 017.
- [26] A. Bandyopadhyay, S. Choubey, S. Goswami, K. Kar, *Impact of the first SNO results on neutrino mass and mixing*, *Phys. Lett. B* **519** (2001) 83; A. Bandyopadhyay, S. Choubey, S. Goswami, K. Kar, *Three generation neutrino oscillation parameters after SNO*, *Phys. Rev. D* **65** (2002) 073031 [hep-ph/0110307].
- [27] J.N. Bahcall, P.I. Krastev, A.Yu. Smirnov, *Solar neutrinos: global analysis and implications for SNO*, *J. High Energy Phys.* **05** (2001) 015 [hep-ph/0103179].
- [28] M.C. Gonzalez-Garcia, M. Maltoni, C. Peña-Garay, J.W.F. Valle, *Global three-neutrino oscillation analysis of neutrino data*, *Phys. Rev. D* **63** (2001) 033005 [hep-ph/0009350].
- [29] J.N. Bahcall, P.I. Krastev, A.Yu. Smirnov, *Where do we stand with solar neutrino Oscillations?*, *Phys. Rev. D* **58** (1998) 096016.
- [30] G.L. Fogli and E. Lisi, *Standard solar model uncertainties and their correlations in the analysis of the solar neutrino problem*, *Astropart. Phys.* **3** (1995) 185 with updated uncertainties as discussed in G.L. Fogli, E. Lisi, D. Montanino, A. Palazzo, *Three-flavor MSW solutions of the solar neutrino problem*, *Phys. Rev. D* **62** (2000) 013002.
- [31] G.L. Fogli, E. Lisi, D. Montanino, *Matter-enhanced three-flavor oscillations and the solar neutrino problem*, *Phys. Rev. D* **54** (1996) 2048.
- [32] A. Gouvea, A. Friedland, H. Murayama, *The dark side of the solar neutrino parameter space*, *Phys. Lett. B* **490** (2000) 125.
- [33] A.J. Baltz and J. Weneser, *Matter oscillations: neutrino transformation in the sun and regeneration in the earth*, *Phys. Rev. D* **37** (1988) 3364.
- [34] M.C. Gonzalez-Garcia, C. Peña-Garay, A.Yu. Smirnov, *Zenith angle distributions at Super-Kamiokande and SNO and the solution of the solar neutrino problem*, *Phys. Rev. D* **63** (2001) 113004.
- [35] A. Friedland, *MSW effects in vacuum oscillations*, *Phys. Rev. Lett.* **85**, 936 (2000).

[36] H. Minakata and O. Yasuda, *Constraining almost degenerate three-flavor neutrinos*, *Phys. Rev.* **D 56** (1997) 1692; A. Yu. Smirnov, *Lepton mixing: small, large, maximal?*, hep-ph/9907296; H. Georgi and S.L. Glashow, *Neutrinos on earth and in the heavens*, *Phys. Rev.* **D 61** (2000) 097301; K. Choi, E.J. Chun, K. Hwang, W.Y. Song, *Bi-maximal neutrino mixing and small U_{e3} from Abelian flavor symmetry*, *Phys. Rev.* **D 64** (2001) 113013; A. Ghosal, *Two parameter texture of nearly bimaximal neutrino mixing*, *Phys. Rev.* **D 62** (2000) 092001; Q. Shafi and Z. Tavartkiladze, *Anomalous flavor $U(1)$: predictive texture for bi-maximal neutrino mixing*, *Phys. Lett.* **B 482** (2000) 145; R.N. Mohapatra, A. Pérez-Lorenzana, C.A. de S. Pires, *Type II seesaw and a gauge model for the bimaximal mixing explanation of neutrino puzzles*, *Phys. Lett.* **B 474** (2000) 355; V. Barger, S. Pakvasa, T.J. Weiler, K. Whisnant, *Bi-maximal mixing of three neutrinos*, *Phys. Lett.* **B 437** (1998) 107; C.S. Kim and J.D. Kim, *Hierarchical quark mixing and bimaximal lepton mixing on the same footing*, *Phys. Rev.* **D 61** (2000) 057302; A. Baltz, A.S. Goldhaber, M. Goldhaber, *An oscillation solution with maximal neutrino mixing*, *Phys. Rev. Lett.* **81** (1998) 5730; M. Ježabek and Y. Sumino, *Neutrino mixing and see-saw mechanism*, *Phys. Lett.* **B 440** (1998) 327; G. Altarelli and F. Feruglio, *Neutrino mass textures from oscillations with maximal mixing*, *Phys. Lett.* **B 439** (1998) 112; Z.-z. Xing, *Bimaximal neutrino mixing pattern reexamined*, *Phys. Rev.* **D 61** (2000) 057301; P.H. Frampton and S.L. Glashow, *Can the Zee ansatz for neutrino masses be correct?*, *Phys. Lett.* **B 461** (1999) 95; Y. Koide and A. Ghosal, *Bimaximal neutrino mixing in a Zee-type model with badly broken flavor symmetry*, *Phys. Rev.* **D 63** (2001) 037301; W.G. Scott, *Tri-maximal vs. bi-maximal neutrino mixing*, *Nucl. Phys.* **B 85** (*Proc. Suppl.*) (2000) 177; Y.-L. Wu, *Spontaneous breaking of flavor symmetry and naturalness of nearly degenerate neutrino masses and bi-maximal mixing*, *Sci. China* **A 43** (2000) 988.

[37] The Super-Kamiokande collaboration, Y. Fukuda et al., *Evidence for oscillation of atmospheric neutrinos*, *Phys. Rev. Lett.* **81** (1998) 1562; T. Futagami, et al, *Observation of the east-west anisotropy of the atmospheric neutrino flux*, *Phys. Rev. Lett.* **85** (2000) 3999.

[38] J. Bahcall and P.I. Krastev, *Does the sun appear brighter at night in neutrinos?*, *Phys. Rev.* **C 56** (1997) 2839.

[39] J.N. Bahcall, P.I. Krastev, A.Yu. Smirnov, *SNO: predictions for ten measurable quantities*, *Phys. Rev.* **D 63** (2000) 093004.

[40] J.N. Bahcall, P.I. Krastev, E. Lisi, *Neutrino oscillations and moments of electron spectra*, *Phys. Rev.* **D 55** (1997) 494.

[41] B. Faid, G.L. Fogli, E. Lisi and D. Montanino, *Vacuum oscillations and variations of solar neutrino rates in SuperKamiokande and Borexino*, *Astropart. Phys.* **10** (1999) 93; A. de Gouvea, A. Friedland, H. Murayama, *Seasonal variations of the Be-7 solar neutrino flux*, *Phys. Rev.* **D 60** (1999) 093011; V. Berezinsky,

G. Fiorentini, M. Lissia, *Vacuum oscillations and excess of high energy solar neutrino events observed in Superkamiokande*, *Astropart. Phys.* **12** (2000) 299.